Revista Mexicana de Astronomía y Astrofísica, **48**, 183–197 (2012)

CHEMICAL ABUNDANCES OF LATE-TYPE SPIRAL GALAXIES FROM THE SDSS

A. M. Hidalgo-Gámez, A. Moranchel-Basurto, and A. F. González-Fajardo

Escuela Superior de Física y Matemáticas
Instituto Politécnico Nacional, Mexico

Received 2012 February 8; accepted 2012 March 22

RESUMEN

Se ha determinado la abundancia de oxígeno para una muestra de 15 galaxias espirales tardías, tanto enanas (dS) como Sm normales. Los espectros se han obtenido de la base de datos del SDSS. Excepto tres de estas galaxias, el resto no tiene determinaciones previas de su contenido químico. La línea prohibida del oxígeno a 4363 Å no se pudo detectar excepto para cuatro galaxias. La abundacia para las otras galaxias se determinó usando los métodos semi-empíricos. Los resultados indican que la mayoría de las galaxias dS tienen abundancias menores que la solar mientras que las Sm pueden tener abundancias mayores.

ABSTRACT

Oxygen abundances have been determined for a total of 15 late-type spiral galaxies. The intensities of the emission lines were determined from the spectra retrieved from the SDSS data-base. Only three galaxies have abundances previously reported in the literature. For four of them the forbidden oxygen line was detected in the spectra but the T_e determined for three of them is larger than 20,000 K. The chemical abundances for the other galaxies were determined with semi-empirical methods. The values indicate that, in general, the oxygen abundance of dS galaxies is smaller than for Sm ones.

Key Words: galaxies: abundances — galaxies: spiral — H II regions

1. INTRODUCTION

The existence of dwarf spiral galaxies (dS) has been controversial since the very begining. Reaves (1956) classified four galaxies of the Virgo cluster as dwarf spiral galaxies, although he said that "the existence of these objects has not been established" and their existence "is inferred by analogy with the dwarf variants of normal ellipticals and irregulars". But, the distance to the Virgo Cluster was estimated to be smaller than 3 Mpc at that time. Sandage, Binggeli, & Tammann (1985), from their study of the luminosity function in the Virgo cluster, claimed that although there was previous evidence of small Sm galaxies, none Sa to Sc dwarf galaxy was ever discovered there. Finally, Edmunds & Roy (1993) concluded that a spiral structure could not exist for galaxies less luminous than $M_B = -17$. In spite of this, there are 12 galaxies classified as dwarf spirals in the UGC (Nilson 1973). In later years some dwarf early-type spiral galaxies have been discovered by Schombert et al. (1995), and Hidalgo-Gámez (2004; hereafter HG04) reclassified a total of 111 galaxies late-type spirals, with optical radius smaller than 5 kpc and absolute magnitude lower than −18 as dS.

The properties of these late-type dS were discussed in detail in HG04 in order to see if they were different from the Sm of larger size. Among other results it was found that colors of the dS galaxies were bluer than normal-size Sm but their star formation rates were very low (Reyes-Pérez & Hidalgo-Gámez 2008). Very few of the dS galaxies in the Hidalgo-Gámez sample might be located inside clusters or large groups of galaxies and the number of barred galaxies is lower than among normal Sm galaxies. Few of these dS galaxies show a clear spiral pattern. Instead, torn off arms, not well defined, are observed and most of the time only one arm is detected.

In a previous investigation, Hidalgo-Gámez & Olofsson (2002) determined that the integrated oxy-

gen abundances of Im galaxies were smaller than the abundances of classical Sm galaxies by a factor of 0.2 dex. In recent years, the abundance has been determined for a total of 18 dS galaxies and the results were that most of them have low, or very low, abundances, lower than 12+log(O/H)=8.2, similar to those of Im and slightly smaller than those of Sm galaxies, and only one galaxy, UGC 7861, might have oversolar abundance (see § 6.1). This is not expected because of the *a priori* different star formation histories of these types of galaxies. It is supposed that the star formation (SF) in spiral galaxies is continuous due to the dynamical spiral arms, while it proceeds in bursts, separated by 10^8 years, in Im galaxies (Carroll & Ostlie 2007). Therefore, the metal content should be larger in the former than in the latter, if the same IMF works in both types of galaxies. Moreover, these galaxies seem to have different environments in the sense that irregular galaxies often are companions of normal size spiral galaxies while dS seem to be isolated or in small associations (HG04), which might influence the star formation rates. Therefore, it might be of the utmost importance to understand such a coincidence in the metallicity range between the dS and the irregular galaxies. If this situation still holds when more galaxies are included, different conclusions can be attained: the spiral arms of the Sm and dS might not influence the SF; or the IMF might differ for Im galaxies, favoring the existence of a large number of massive stars, which produce and release heavier elements, as oxygen. Or, all these galaxies are really the same kind of galaxies, and the classification scheme is too detailed. Or, there are some other differences in the evolution of late-type galaxies. Therefore, a larger sample of late-type galaxies with well determined oxygen abundances must be considered before indulging in any further speculation on their evolution.

The main goal of this investigation is to increase the sample of dS galaxies with oxygen abundance determinations in order to verify if there are dS galaxies with oversolar abundances, as any other typical spiral galaxy (Skillman et al. 1996) or all of them have undersolar values, as the Im. The description of the sample used here is presented in § 2 while the analysis of the spectra is given in § 3. In § 4 the different methods for the abundance determination are described and the results on the oxygen abundance for this sample are presented in § 5. Finally, a discussion on some interesting results and a comparison with previous results are given in § 6. Conclusions are outlined in § 7.

2. THE SAMPLE

In order to get a large sample of late-type spiral galaxies with known abundances, the SDSS database[1] was searched. Both, the dS galaxies from the list of HG04 and a comparison sample (hereafter, the Sm sample), which consists of Sm with $r_{25} > 5$ kpc and $M_B < -18$, are cross-correlated with the SDSS database. Only the spectra of those galaxies with information on the equivalent width (EW) of Hβ and Hα lines as well as on the oxygen lines at λ, λ 4959,5007 Å were retrieved. These make up a total of 23 galaxies. When the spectra were analyzed, the Hβ could not be detected in eight of these galaxies, although a positive value of the EW was stated in the data-base. In all these eight galaxies the error associated with the EW(Hβ) values was larger than the canonical value of the EW. Moreover, all these eight spectra were very noisy. For one galaxy, UGC 7780, no emission line could be detected and the spectrum resembles that of a cold star instead of an HII region. Then, these galaxies were not considered for the chemical abundance determination and the final sample consists of a total of 15 galaxies, 7 dS and 8 Sm, which are shown in Table 1. Only three of these galaxies have previous abundance determination: UGCA 294 (Shi et al. 2005), UGCA 322 (Pilyugin & Thuan 2007), and UGC 7861 (Moustakas et al. 2010). They are included here for the sake of completeness and comparison.

2.1. *The dS sample*

As previously said, a total of seven dwarf spiral galaxies have been studied here. Their main characteristics are summarized in Table 1. From it, it is clear than UGC 6205 and UGC 9597 are among the largest galaxies in the dS sample but they are not very bright. UGC 9597 is located in a small association with two more galaxies (Garcia 1993) while UGC 6205 seems to be isolated. Its gas mass is $0.45\times10^9\ M_\odot$ and the number of HII regions is small; only 9 regions were detected in the Hα image (Reyes-Pérez 2009). The spiral structure of this galaxy does not show any disturbance in any of the bands (V, R and Hα) observed. UGC 8285 is also located in a small association (Fouqué et al. 1992) and it is also large as compared with the average dS population.

[1]Funding for the SDSS and SDSS-II was provided by the Alfred P. Sloan Foundation, the Participating Institutions, the National Science Foundation, the U.S. Department of Energy, the National Aeronautics and Space Administration, the Japanese Monbukagakusho, the Max Plank Society, and the Higher Education Funding Council for England. The SDSS was managed by the Astrophysical Research Consortium for the Participating Institutions.

TABLE 1

CHARACTERISTICS OF THE GALAXIES IN THE SAMPLE

Galaxy	D	r_{25}	M_B	M(HI)	ρ_s	Barred
	Mpc	kpc arcmin^{-1}	...	(10^9 $M_\odot$)	($M_\odot$ kpc^{-2})	...
UGCA 294	9.7	1.02/0.7×0.4	−14.9	0.12	36.7	No
UGC 9018	6.4	1.54/1.7×1.3	−14.7	0.13	17.45	No
UGC 7861	8.2	2.61/1.27×1.2	−16.7	0.49	22.9	X
UGC 8285	26.4	4.32/1.7×0.4	−16.7	0.52	8.87	No
UGC 9597	23.1	4.75/0.93×0.4	−15.3	—	—	No
UGC 5242	24.8	4.86/0.77×0.4	−16.6	0.80	10.8	B
UGC 6205	18.9	4.99/1.8×1.4	−16.5	0.45	3.96	No
UGC 6399	17	6.81/2.5×0.6	−17.03	0.69	4.74	No
UGC 3947	52.2	6.93/0.6×0.4	−16.79	1.35	8.95	No
UGC 9452	29	7.32/0.77×0.3	−16.9	—	—	No
UGC 9381	40.4	8.1/0.44×0.3	−16.1	2.07	10.0	No
NGC 3669	31.5	10.25/0.77×0.55	−19.5	5.34	16.2	B
UGC 1693	52	11.4/3.5×2.6	−16.96	—	—	No
UGCA 322	25	12.9/2.2×0.5	−19.22	6.70	12.8	X
NGC 5630	41.3	13.44/2.05×0.65	−19.6	5.15	9.07	No

In Column 1 the name of the galaxy is listed while the distance, the optical radius and the absolute magnitude are listed in Columns 2, 3, and 4. The HI mass and its surface density, determined as explained in HG04, are shown in Columns 5 and 6. Finally, Column 7 shows if the galaxy is barred (B), weak barred (X) or it has no bar (No).

On the contrary, UGC 9018, UGC 7861 and UGCA 294 are small galaxies. UGC 7861 is a low-luminosity, small galaxy in interaction with NGC 4618. In spite of this interaction, the HI velocity field and the rotation curve of the galaxy are regular and well-defined (Gil de Paz et al. 2005). Recently, an extended UV emission, four times larger than the optical disk, has been detected on the top of the low surface brightness optical disk (Gil de Paz et al. 2007). UGCA 294 is the smallest galaxy in the present sample, with an optical radius of 1.02 kpc at a distance of 9.7 Mpc (HG04). Despite its low absolute magnitude, it is classified as BCG (Kong & Cheng 2002). UGC 9018 is as tiny as UGCA 294 (r_{25} = 1.02 kpc, HG04), and dim (M_B = −14.90, HG04). It is located in an association along with other four galaxies (Garcia 1993).

Finally, UGC 5242 is a barred galaxy with an optical size, at the 25th isophote, of 4.86 kpc and located at a distance of 24.7 Mpc (HG04). Despite being in the Vorontson-Velyaminov catalogue (1974), it is not classified as a peculiar or interacting galaxy. It does not show disturbances in its morphology, although the spiral structure is not very well defined, as is clearly seen in the optical images provided by SDSS.

2.2. *The Sm sample*

The eight galaxies in the Sm subsample are less heterogeneous, as can be seen in the second part of Table 1. Half of them are not very large, and not very bright (for being non-dwarf). One of them, UGC 9381, is classified as a non-dwarf candidate by Whiting et al. (2007) in their survey of the dwarf galaxy population of the Local Group. This is quite surprising because none of the galaxies in the Sm subsample are really nearby, the closest one being located further than the Virgo Cluster. In addition to being smaller, these four galaxies have less gas mass than the other, larger, Sm galaxies. Two of them are located inside small galaxy associations (Garcia 1993), with another three galaxies (NGC 3996), and seven galaxies (UGC 1693). On the contrary, UGCA 322 is listed in the AMIGA catalog, an indication of its isolation. Only NGC 3669 is classified as strong barred, while UGCA 322 is considered as weak barred (de Vaucouleurs et al. 1991).

3. ANALYSIS OF THE SPECTRA

The calibrated spectra for all the galaxies were retrieved from the SDSS data-base and analyzed by the authors. All these spectra pertain to the center

part of the galaxies except for two of the galaxies for which the spectra are slightly off-centered. As the SDSS fiber size is $3''$ and the smallest angular size is $30''$, they all covered a tiny part of the galaxies. For four galaxies more than two spectra are marked in the image, but only one can be retrieved. In those case, it is supposed that those spectra stem from the centered fiber.

In order to analize these spectra the authors used the subroutine ALICE with the MIDAS software. The emission lines were detected by eye and fitted with the INTEGRATE command. All the lines were measured twice, except when the measurements differed by more than 50%. In this case, a third value was obtained. The quality of these spectra is very heterogeneous. Some of them have very good S/N, as UGC 9018, while in most of them the S/N ratio diminishes towards the blue part of the spectra, making difficult the detection of the lines of this part of the spectra, including Hβ. The INTEGRATE command gives both the total flux in the line and the equivalent width and the continuum. Therefore, two different measurements of the flux can be obtained. They can be compared and their differences can be computed as part of the uncertainties in the intensity, the so-called σ_f (see below). From these two sets of fluxes, an averaged value was determined for each of the lines. The usual procedures of normalization and correction were applied to these values. The extinction correction was performed using the extinction coefficient defined as (Aller 1984)

$$C_\beta = \frac{1}{f(\lambda)} \ln \frac{F(\mathrm{H}\alpha)/F(\mathrm{H}\beta)}{2.86}\,, \qquad (1)$$

where 2.86 is the theoretical I(Hα)/I(Hβ) ratio at 10000 K for case B of recombination (Brocklehurst 1971), $f(\lambda)$ is the Whitford modified extinction law (Savage & Mathis 1979), and $F(\mathrm{H}\alpha)/F(\mathrm{H}\beta)$ is the observed Hα/Hβ ratio. Five galaxies show an observed Balmer decrement smaller than the theoretical one: UGCA 294, UGC 9597, UGC 9018, UGCA 322 and UGC 9452. There must be several reasons for such values. Firstly, we checked the extinction using another software (Dypso at STARLINK), just to verify if this could be a problem of the fitting of the lines or the continuum. However, the same result was obtained with the intensities determined with Dypso, with a Balmer decrement smaller than the theoretical. Therefore, this should be real and not an artifact of the software used.

A wrong Balmer decrement must be an indication of an odd flux calibration. As the data were calibrated from the SDSS group and we retrieved the complete reduced and calibrated data sets, this cannot be avoided. The flux calibration performed by the SLOAN team can be checked from the ratio of the lines [OIII]λ5007/[OIII]λ4959 and [NII]λ6583/[NII]λ6548. Both ratios should be about 3. It can be determined from Tables 2 and 3 than these values are about 3, as expected, for these five galaxies. Therefore, the flux calibration cannot be responsible for the small Balmer decrement of these galaxies unless the flux calibration is wavelength-dependent, which is very unlikely.

Another situations can be invoked, namely scattered light which increased the intensities of the blue lines, particularly the Hβ intensity (O'Dell et al. 2011) or a loss of Hα intensity because of differential refraction or a similar problem. In order to check these values, other Balmer lines were considered when detected. In one galaxy, UGCA 322, the observed Hγ/Hβ and Hδ/Hβ ratios are exactly the theoretical ones. This could be an indication that the blue light is more intense than the red one. Then, a different approach were considered. We decided to fix the Hα/Hβ ratio to 2.86 for all these five galaxies, and determined the Hβ intensity from it. As we said before, the S/N decreased towards the blue part for all the spectra; then the Hβ intensity is always more uncertain than the Hα one. With this new Hβ intensity, a new set of normalized intensities was obtained. These values will be used in the abundance determination.

Finally, the uncertainties were determined from the sum in quadrature of the Poisson noise (σ_c), the extinction correction (σ_e), and the differences in the flux determinations as described above (σ_f), using the following expression

$$\sigma = \sqrt{(\sigma_c)^2 + (\sigma_e)^2 + (\sigma_f)^2}\,.$$

4. ON THE OXYGEN ABUNDANCE DETERMINATION

The final value of the intensities are listed in Table 2 for dS galaxies and in Table 3 for Sm ones. It can be seen that the oxygen forbidden line [OIII]λ4363 is detected in four galaxies and the standard method can be used to determine the abundance (e.g., Osterbrock 1989). The main caveat is that the intensity of this line, normalized to Hβ, is quite large for UGCA 322. As this is not the usual situation because normally [OIII]λ4363/Hβ is of the order of 0.05 (see the classical work of McCall, Rybski, & Shields 1985), the standard method is not used for this galaxy. It is interesting to notice than the

TABLE 2

CORRECTED INTENSITIES OF THE EMISSION LINES OF THE dS GALAXIES IN THE SAMPLE

Line	UGC 7861	UGCA 294	UGC 8285	UGC 9597	UGC 5242	UGC 6205	UGC 9018
[OII] λ3727	0.9±0.4	2±1	3±1	1.7±0.5	3±1	3±1	1.7±0.8
H11 λ3771	···	···	···	···	···	···	0.062±0.001
H10 λ3798	···	···	···	···	···	···	0.099±0.001
[NeIII] λ3869	···	···	···	···	···	···	0.537±0.007
He I λ3889	···	···	···	···	···	···	0.301±0.004
[NeIII] λ3970+H7	···	···	···	···	···	···	0.387±0.005
Hδ	···	···	···	···	···	···	0.383±0.005
Hγ	···	0.45±0.05	···	···	0.65±0.09	···	0.636± 0.007
[OIII] λ4363	···	0.15±0.09	···	···	0.15±0.02	···	0.084±0.001
He I λ4471	···	···	···	···	0.13±0.03	···	0.053±0.001
[ArVI] λ4711	···	···	···	···	···	···	0.007±0.001
Hβ	1.00±0.02	1.00±0.07	1.00±0.03	1.0±0.4	1.0±0.1	1.0±0.1	1±0.01
[OIII] λ4959	0.34±0.03	1.3±0.1	0.51±0.07	0.40±0.01	0.74±0.09	0.7±0.1	1.87±0.02
[OIII] λ5007	0.99±0.08	3.7±0.2	1.6±0.1	1.39±0.05	2.5±0.3	2.7±0.3	5.1±0.1
[ClIII] λ5517	···	···	···	···	···	···	0.005±0.0001
[ClIII] λ5530	···	···	···	···	···	···	0.004±0.0001
He I λ5875	···	0.16±0.01	···	···	0.15±0.02	···	0.119±0.002
[OI] λ6301	···	0.061±0.004	···	···	0.10±0.01	···	0.015±0.001
[SIII] λ6312	···	···	···	···	···	···	0.020±0.0001
[OI] λ6363	···	0.039±0.03	···	···	···	···	0.007±0.001
[NII] λ6548	···	0.026±0.002	0.087±0.005	···	0.07±0.001	···	0.018±0.005
Hα	2.86±0.07	2.86±0.2	2.86±0.1	2.86±0.05	2.86±0.3	2.86±0.3	2.86±0.03
[NII] λ6583	2.00±0.04	0.12±0.03	0.35±0.09	0.40±0.01	0.22±0.03	0.70±0.08	0.055±0.001
He I λ6678	···	···	···	···	···	···	0.027±0.0001
[SII] λ6717	0.92±0.03	0.31±0.02	0.65±0.04	0.56±0.06	0.49±0.06	0.8±0.1	0.094±0.002
[SII] λ6731	0.67±0.01	0.24±0.02	0.43±0.03	0.52±0.02	0.35±0.04	0.53±0.07	0.068±0.001
He I λ7065	···	···	···	···	···	···	0.018±0.0005
[ArIII] λ7136	···	···	···	···	···	···	0.074±0.002
He I λ7281	···	···	···	···	···	···	0.005±0.001
[OII] λ7320	···	···	···	···	···	···	0.021±0.0003
[OII] λ7330	···	···	···	···	···	···	0.017±0.0001
He I λ7499	···	···	···	···	···	···	0.013±0.001
[SIII] λ9065	···	···	···	···	···	···	0.144±0.005
Cβ	2.09±0.05	0.00	0.65±0.03	0.00	0.31±0.04	1.2±0.1	0.00
S/N (5007)	2.5	186	17	3.4	75	11	1378

The identification of the line is given in Column 1 while the names of the galaxies are given in Column 2 to 8. The extinction Balmer coefficient and the S/N in the vicinity of Hβ are given in the last two rows for each galaxy. See text for the detailed explanation of the determination of the uncertainties.

forbidden oxygen line [OIII]λ4363 equivalent width is provided by the SDSS data-base for another three galaxies of this sample. In all these galaxies the EW of the line is smaller than its uncertainty, or the flux of the line is larger than the flux of Hβ. We were very careful when these three galaxies were analyzed to look for this line but it could not be detected in any of them. As the SDSS analysis procedure is quite automatic we think that this information does not correspond to any emission line, but it is due to noise, and we did not consider such intensities in this investigation.

In any case, the main caveat with these data is that the oxygen lines [OII]λ, λ3726,3729 (hereafter [OII]λ3727) are not detected for any of the studied galaxies, mainly because these are nearby objects and the wavelength coverage of the SDSS starts at 3800 Å. This is quite troublesome, because without the intensity of this line the oxygen abundance relies on only two semi-empirical methods. In some other investigations (e.g., Kniazev et al. 2004) the oxygen lines at λ, λ7320,7330 Å were used, but such lines are also absent for most of the galaxies in this sample. Therefore, it might be interesting to find a way to ob-

TABLE 3

FLUXES, ABSORPTION AND EXTINCTION CORRECTED, OF THE EMISSION LINES OF THE Sm GALAXIES IN THE SAMPLE

Line	NGC 3669	NGC 5630	UGC 1693	UGC 6399	UGC 9381	UGCA 322	UGC 3947	UGC 9452
[OII] λ3727	0.8±0.2	0.6±0.2	1.3±0.9	0.19±0.07	3±1	2.8±0.9	2±1	3±1
He I λ3889	···	···	···	···	···	0.18±0.01	···	···
[NeIII] λ3970	···	···	···	···	···	0.13±0.01	···	···
Hδ	0.30±0.04	0.19±0.07	···	···	···	0.25±0.03	···	···
Hγ	0.50±0.04	0.4±0.1	···	···	···	0.58±0.01	···	0.57±0.08
[OIII] λ4363	···	···	···	···	···	0.88±0.01	···	···
Hβ	1.00±0.1	1.0±0.3	1.0±0.2	1.0±0.04	1.0±0.1	1.00±0.01	1.0±0.3	1.00±0.02
[OIII] λ4959	0.15±0.04	0.23±0.08	0.4±0.1	0.19±0.07	1.0±0.1	0.888±0.003	0.5±0.1	1.00±0.04
[OIII] λ5007	0.89±0.02	0.9±0.3	1.2±0.3	0.6±0.2	3.0±0.3	2.62±0.03	1.8±0.5	3.05±0.1
He I λ5875	···	0.09±0.03	···	···	···	0.137±0.003	···	0.18±0.02
[OI] λ6301	0.09±0.04	0.12±0.04	···	···	···	0.073±0.002	···	0.15±0.02
[SIII] λ6312	···	···	···	···	···	0.032±0.002	···	···
[OI] λ6330	···	0.03±0.01	···	···	···	0.027±0.003	···	0.12±0.01
[NII] λ6548	0.23±0.04	0.19±0.06	···	···	···	0.088±0.003	···	···
Hα	2.86±0.06	2.86±0.9	2.86±0.7	2.86±1	2.86±0.3	2.86±0.04	2.86±0.7	2.86±0.1
[NII] λ6583	0.75±0.04	0.7±0.2	0.6±0.1	0.7±0.2	0.40±0.06	0.282±0.004	0.7±0.2	0.27±0.02
He I λ6678	···	···	···	···	···	0.036±0.001	···	···
[SII] λ6717	0.74±0.04	0.6±0.2	1.1±0.2	1.2±0.4	···	0.415±0.003	1.0±0.3	0.42±0.02
[SII] λ6731	0.54±0.04	0.5±0.1	0.7±0.2	0.6±0.2	···	0.290±0.002	0.7±0.2	0.31±0.01
[OII] λ7320	···	···	···	···	···	0.024±0.002	···	···
[OII] λ7330	···	···	···	···	···	0.026±0.006	···	···
Cβ	0.47±0.04	0.17±0.05	1.13±0.2	0.3±0.1	2.2±0.2	0.0	0.6±0.1	0.00
S/N(5007)	15	31	7	3	5	335	30	43

The identification of the line is given in Column 1, the names of the galaxies are given in Column 2 to 8. The extinction Balmer coefficient and the S/N in the vicinity of Hβ are given in the last two rows for each galaxy. See text for the detailed explanation of the determination of the uncertainties.

tain information on the intensity of the [OII] doublet. This could be done through the relationship between the intensities of [OIII]λ5007 Å and [OII]λ3727 Å. Such a relationship can be obtained directly from photoionization models (Martín-Manjón et al. 2008) and it has been used as a diagnostic diagram (e.g., Baldwin, Phillips, & Terlevich 1981). In the present investigation, we used the relationship obtained from a sample of 438 star-forming galaxies studied by Kniazev et al. (2004) from the DR1-SDSS. For a complete description of this sample the reader is referred to Hidalgo-Gámez & Ramírez-Fuentes (2009). Such a relationship, which is shown in Figure 1, follows the equation

$$\log \frac{[\mathrm{OII}]}{\mathrm{H}\beta} = -2.82 \left(\log \frac{[\mathrm{OIII}]}{\mathrm{H}\beta}\right)^2 + 2.39 \log \left(\frac{[\mathrm{OIII}]}{\mathrm{H}\beta}\right) - 0.0542\,, \qquad (2)$$

with a rather large dispersion, of around 35%, for values between $0.8 > \log[\mathrm{OIII}]\lambda5007/\mathrm{H}\beta > 0.6$, but smaller outside this range. Kobulnicky, Kennicutt, & Pizagno (1999) proposed a similar procedure for high redshift galaxies, for which the oxygen line [OIII]λ5007 is not detected. They did not give any equation to compare it with but they obtained a similar plot in both shape and dispersion to the one in Figure 1. Although the dispersion of such a relationship is large, a value for the intensity of the [OII]λ3727 can be obtained and, therefore, the abundances for all the HII regions can be determined. In order to check how reliable the abundances determined with these intensities are, several tests were performed. First, the intensity of the oxygen lines measured from the spectra were compared to the intensities determined from equation 2 for the galaxies from Kniazev et al. Although the values are very similar, still there are some discrepancies. The next step is to compare the standard method abundance determined with both sets of [OII]λ3727 line intensities (Figure 2). The differences between them are smaller than the canonical uncertainty of the sample, which is about 0.08 dex (Hidalgo-Gámez &

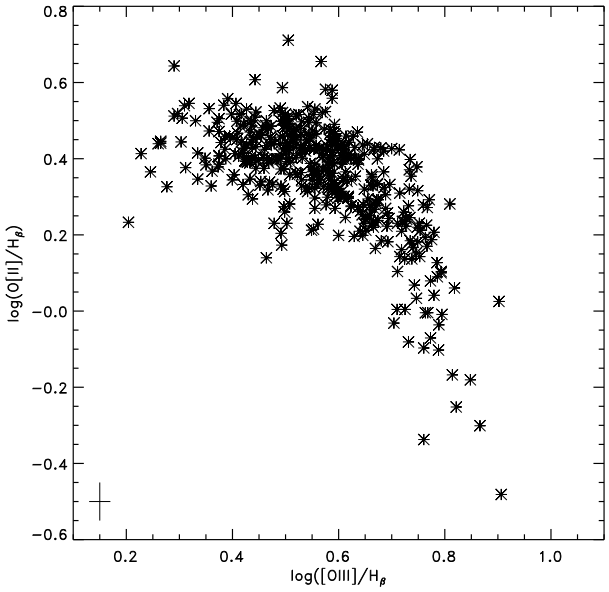

Fig. 1. The [OII]/Hβ vs. [OIII]/Hβ intensities from a sample of 438 star-forming galaxies. The largest dispersion is found in the range $0.4 < \log([\mathrm{OIII}]/\mathrm{H}\beta) < 0.6$, and is about 35%.

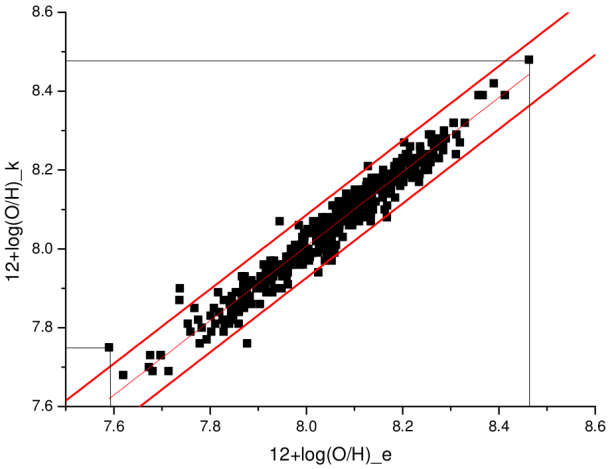

Fig. 2. Comparison of the abundances determined with the [OII] intensities obtained from equation 2 vs. the abundances determined with the [OII] intensities measured from the spectra. The thick lines are the typical uncertainties around the value (see text for details).

Ramírez-Fuentes 2009). This is also true when the semi-empirical methods (R_{23} and P) are used for the abundance determination. Then, it can be concluded that although the uncertainties in the [OII]λ3727 line might be larger than the usual ones, the abundances determined from these values are quite correct.

Once the intensity of the [OII]λ3727 Å line was obtained the abundances were determined. As previously said, the oxygen abundance has to be determined with the semi-empirical methods for 12 of the galaxies while the standard method can be used for only three of them. The expressions by Aller (1984) were used in the determination of the electron temperature and the oxygen abundance. Concerning the semi-empirical methods, four different ones were used here to determine the oxygen abundances: the R_{23} proposed by Pagel et al. (1979) and lately calibrated by McGaugh based on his photoionization models and given by Kobulnicky et al. (1999) as

$$Z_l = 12 - 4.944 + 0.767x + 0.602x^2 - y(0.29 + 0.332x - 0.331x^2)\,, \quad (3)$$

$$Z_u = 12 - 2.939 - 0.2x - 0.237x^2 - 0.305x^3 - 0.0283x^4 - y(0.0047 - 0.0221x - 0.102x^2 - 0.0817x^3 - 0.00717x^4), \quad (4)$$

for the low and the high metallicity branch, respectively, with $y = \log([\mathrm{OIII}]5007 + [\mathrm{OIII}]4959)/([\mathrm{OII}]3727)$ and $x = \log\ R_{23}$. The second method used is the so-called P method, as calibrated by Pilyugin & Thuan (2005), with the following equations for the low and high metallicity branches

$$Z_u = \frac{R_{23} + 726.1 + 842.2P + 337.5P^2}{85.96 + 82.76P + 43.98P^2 + 1.793R_{23}}\,, \quad (5)$$

$$Z_l = \frac{R_{23} + 106.4 + 106.8P - 3.4P^2}{17.72 + 6.6P + 6.95P^2 - 0.302\ R_{23}}\,, \quad (6)$$

with $P = ([\mathrm{OIII}]5007 + [\mathrm{OIII}]4959)/([\mathrm{OII}]3727)$. The next one is the $O3N2$ method, based on the correlation between the oxygen and nitrogen most brightest lines ratio and the oxygen abundances (Pettini & Pagel 2004) and is given by

$$12 + \log(\mathrm{O/H}) = 8.73 - 0.32\ O3N2\,, \quad (7)$$

with $O3N2$ defined as $\log \frac{([\mathrm{OIII}]/\mathrm{H}\beta)}{([\mathrm{NII}]/\mathrm{H}\alpha)}$.

Finally, the $N2$ method is based on the relationship between the oxygen abundance and the [NII]/Hα ratio and was calibrated by Denicoló, Terlevich, & Terlevich (2002) as

$$12 + \log(\mathrm{O/H}) = 9.12 + 0.73\ N2\,, \quad (8)$$

with $N2$ defined as $\frac{\log [\mathrm{NII}]}{\mathrm{H}\alpha}$.

One of the problems with two of these semi-empirical methods is that they are bi-valuated. This means that there are two zones of metallicity for the same value of the R_{23} value, the so-called low-metallicity and high-metallicity branches (Edmunds

& Pagel 1984). As the abundances are determined from different equations for the low and the high branches, an *a priori* criterion is needed in order to determine in which of these two regions the abundance of the HII region studied is. The most widely used criterion is based on the log([NII]/[OII]) ratio. When this ratio is higher than −1.0, the region is considered of high metallicity. One might think that considering the uncertainties in the [OII] intensities, this ratio could be lower (or higher) than −1.0 and the region might be on the high (or low) metallicity branch. In this sense, the abundances determined with the $N2$ and the $O3N2$ methods were a guess on the metallicity branch and in most of the cases the values agreed with the ones determined from the log([NII]/[OII]) ratio. Following Pilyugin & Thuan (2005), the separation between the two branches is at 8.2 dex.

Another concern about the semi-empirical methods is their dependence on other parameters beside the oxygen abundances, such as the ionization temperature (Olofsson 1997), or the nitrogen content for those relying on the intensity of the nitrogen lines (Stasińska 2008). The dependence on the ionization parameter has been studied, among others, by McGaugh (1991) and in the expression used here such dependence is taken into account through the y parameter. Pilyugin (2001) said that the P parameter takes into account the ionization parameter. Therefore, the abundance determinations provided here should not be ionization parameter dependent. Another problem affecting only the $O3N2$ calibration is that it is saturated near the solar abundance (Erb et al. 2006) and, it might not be very reliable for larger abundances.

In Hidalgo-Gámez & Ramírez-Fuentes (2009), the accuracy of two of these methods was studied. They focused on the R_{23} and the P methods because their sample did not include the intensities of the nitrogen lines. Their main conclusion was that although the new calibration of the P method gives values of the metallicity closer to those obtained with the standard method in general and with lower dispersion, there are other problems such as the bimodal distribution of the abundance (see Figure 2 in Hidalgo-Gámez & Ramírez-Fuentes 2009), the discontinuity in the abundance (see Figure 4 in Hidalgo-Gámez & Ramírez-Fuentes 2009) and the fact that between 7.95 dex and 8.2 dex the P method is undefined, which makes the P method not completely favored there. For a deeper discussion on this issue, the reader is referred to the original paper by Hidalgo-Gámez & Ramírez-Fuentes (2009). The precision of the $O3N2$ and $N2$ methods was not studied by Hidalgo-Gámez & Ramírez-Fuentes (2009), as previously said, and we are going to relay on the results by Denicoló et al. (2002) and Pettini & Pagel (2004), respectively. The typical uncertainty is, in both cases, about 0.2 dex. In spite of all their caveats and dependences, the semi-empirical methods are widely used in chemical abundance determinations of spiral galaxies (e.g., Skillman et al. 1996; Márquez et al. 2002).

Therefore, all together, up to five different abundances are available for all the galaxies in the sample and a reliable value can be inferred from them. The uncertainties in the oxygen abundances were obtained from the uncertainties in the line intensities. New values of the abundances were computed using the intensity+uncertainty for each line. The difference between these two values is considered as the uncertainty, and is shown in Table 4 after the nominal abundance value. These uncertainty values are increased with the statistical dispersion of each method, giving a final uncertainty which is shown in parentheses in Table 4. For the R_{23} and the P methods we follow Table 2 in Hidalgo-Gámez & Ramírez-Fuentes (2009), while for both the $N2$ and the $O3N2$ such dispersion is quoted as 0.2 dex, as previously said.

5. RESULTS

The oxygen abundances determined with the semi-empirical methods are shown in Columns 2, 3, 4, and 5 of Table 4 along with the dispersion among them (Column 6). In Column 7 the oxygen abundances determined with the standard method are listed.

The first interesting result from Table 4 concerns the abundances determined with the standard method (hereafter, the standard abundances). All of them have very low values, but for UGC 9018. However, for UGCA 322 the abundance could not be determined as the high intensity of the [OIII]λ4363 line gives a negative electron temperature. The values for UGC 5242 and UGCA 294 are not reliable because they are very low, mainly due to the low S/N of the spectra at this wavelength. UGC 9018 is the galaxy with the largest S/N of the sample, and the lines were very well outlined. In this case the standard abundance is very similar to the values determined with the semi-empirical methods (hereafter, the semi-empirical abundances).

Concerning the semi-empirical abundances, it is very interesting to see that there are important differences in the values. In Column 6 of Table 4 the dispersion among the semi-empirical abundances (σ)

TABLE 4

OXYGEN ABUNDANCE FOR THE GALAXIES IN THE SAMPLE

Galaxy	R_{23}	P	$N2$	$O3N2$	σ	Standard
UGCA 294	8.0±0.3 (0.3)	8.1±0.1 (0.2)	8.1±0.05 (0.2)	8.1±0.03 (0.2)	0.04	7.1±0.1
UGC 9018	8.1±0.1 (0.3)	8.0±0.2 (0.3)	7.87±0.02 (0.2)	7.95±0.01 (0.2)	0.08	8.00±0.1
UGC 5242	8.0±0.1 (0.3)	7.9±0.2 (0.3)	8.3±0.2 (0.4)	8.2±0.2 (0.4)	0.15	6.89±0.09
UGC 7861	8.93±0.06 (0.2)	8.7±0.1 (0.2)	9.00±0.01 (0.2)	8.68±0.01 (0.2)	0.1	···
UGC 9597	8.86±0.04 (0.3)	8.6±0.1 (0.2)	8.5±0.1 (0.3)	8.4±0.1 (0.2)	0.2	···
UGC 8285	8.67±0.05 (0.2)	8.2±0.1 (0.2)	8.45±0.01 (0.2)	8.37±0.02 (0.2)	0.2	···
UGC 6205	8.6±0.1 (0.3)	8.3±0.1 (0.2)	8.67±0.07 (0.3)	8.40±0.05 (0.2)	0.15	···
UGCA 322	8.0±0.2 (0.3)	8.3±0.1 (0.3)	8.39±0.01 (0.2)	8.30±0.01 (0.2)	0.15	···
UGC 9452	8.1±0.1 (0.2)	8.0±0.2 (0.3)	8.38±0.04 (0.2)	8.25±0.02 (0.2)	0.14	···
UGC 9381	8.6±0.1 (0.3)	8.3±0.1 (0.2)	8.50±0.08 (0.3)	8.30±0.06 (0.2)	0.1	···
UGC 3947	8.7±0.1 (0.3)	8.4±0.2 (0.3)	8.7±0.1 (0.3)	8.4±0.1 (0.3)	0.06	···
UGC 1693	8.9±0.1 (0.3)	8.6±0.2 (0.3)	8.6±0.1 (0.3)	8.5±0.1 (0.3)	0.15	···
NGC 5630	9.0±0.05 (0.2)	8.8±0.05 (0.2)	8.68±0.08 (0.2)	8.56±0.04 (0.2)	0.15	···
NGC 3669	9.0±0.03 (0.2)	8.77±0.06 (0.1)	8.69±0.04 (0.2)	8.6±0.56 (0.2)	0.15	···
UGC 6399	9.06±0.04 (0.2)	8.9±0.4 (0.5)	8.7±0.2 (0.4)	8.6±0.1 (0.3)	0.2	···

The name of the galaxy is listed in Column 1, while the abundances obtained with the semi-empirical methods are listed in Columns 2 to 5 along with the uncertainties derived from the uncertainties in the line intensities. In parentheses is given the total uncertainty, where the statistical uncertainties for each method are considered (See text for details). Columns 6 shows the dispersion among all the previous values. Finally, for those galaxies where the abundance could be determined with the standard method, the values are shown in Column 7.

is listed. The dispersion is larger than 0.1 for all except three galaxies. Actually, UGCA 322 has a difference of 0.39 between the highest and the lowest abundance value. Thus, it is very difficult to get a single value of the oxygen abundance.

Another interesting result is that there is no clear pattern in the abundances, in the sense that the values determined with one particular method are always the highest or the lowest. In the values of Table 4, the R_{23} gives the highest abundance for nine out of the 15 galaxies, but for one galaxy it is the lowest. Therefore, it cannot be concluded that the R_{23} abundances are the highest. The only statement that can be made is that neither the P method nor the $O3N2$ one gives the highest abundance for any galaxy. In the case of the $O3N2$ method the value is quite reasonable because it is saturated for oversolar values. Then, this value is just an lower limit for four of the galaxies (UGC 7861, NGC 5630, NGC 3669, and UGC 6399) which have clearly supersolar abundances. It would be very interesting to know the spectral characteristics of the galaxy for which the R_{23} method is an upper limit, but this is out of the scope of this investigation.

Considering this, it is very difficult to say which metallicity a galaxy has. The only thing that can be said is that five out of 15 galaxies have at least three out of the four values of abundances similar or lower than the LMC abundance (Rodriguez & Rubin 2003), four out of 15 have real oversolar abundances and the other six galaxies have abundances between the solar range and the LMC. Although these abundance ranges can be large and undetermined, the interesting point is that such abundances are quite robust in the sense that they are not affected by the extinction (or absorption) corrections or any other procedures. Actually, the difference between the oxygen abundances for the five galaxies with troublesome Balmer decrements only differ in the second decimal value, compared with the non-extinction corrected ones. The results for the oxygen abundances are interesting because for all the galaxies presented in this investigation, the abundances are obtained from the center of them, according to the information provided by the SDSS, where the higher abundance is expected. Therefore, and considering the existence of (steep) abundance gradients in dS galaxies (Hidalgo-Gámez & González, in prepa-

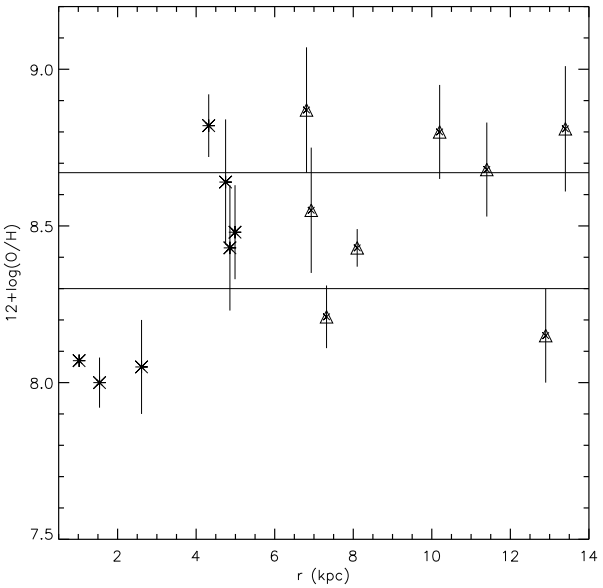

Fig. 3. Oxygen abundance vs. the optical size of the galaxies studied in the present investigation. The triangles are the Sm galaxies and the stars the dS ones. The solar and LMC metallicities are shown as horizontal solid lines. It is clear that the majority of the dS galaxies have subsolar abundance, while most of the Sm galaxies have solar and oversolar abundances.

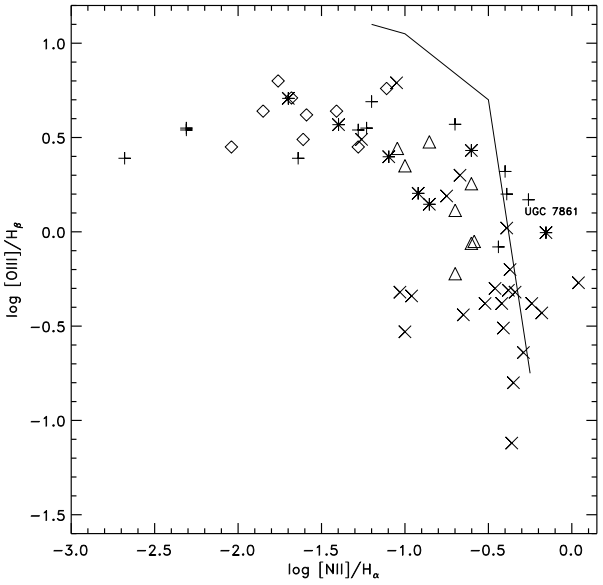

Fig. 4. The [OIII]/Hβ vs. [NII]/Hα diagram for late-type galaxies. The galaxies studied in this investigation are presented as star symbols (dS) and triangles (Sm). Crosses are the Sp galaxies from McCall et al. (1985), while diamonds are Im galaxies and plus signs are dS from the literature (see text for references).

ration), the average values should be even lower than those obtained here.

The other interesting result is that the number of low-metallicity galaxies, being those galaxies with abundances similar to, or lower than, the abundance of the LMC, is very similar for both samples. On the contrary, the number of dS galaxies with oversolar abundances is small, (just one galaxy, UGC 7861) while four out of eight Sm galaxies have oversolar abundances. Actually, UGC 7861 might not be a good example, because although it is classified as a star-forming galaxy, its [NII]/Hα ratio is larger than that for the other star-forming galaxies (see next section). This result is shown in Figure 3, where a representative oxygen abundance for each galaxy (just considered for the sake of clarity without any other purpose) is plotted against the optical radius of the galaxies. The LMC and solar metallicities are shown as horizontal solid lines. The result is similar when other abundances are considered, as can be inferred from Table 4. The main differences are those of the R_{23} abundances, which give a large number of dS galaxies with oversolar abundances and those of the $O3N2$ which give a lower number of galaxies with undersolar abundances, as expected. It is clear from this figure that dS galaxies are, in general, less metallic than Sm ones. This result is similar to what was previously found, namely, that the majority of the dS galaxies have low abundances (see next section). Note that no abundance determination method yields really high values of oxygen for the galaxies studied here (as is the case e.g. for the galaxies in the Virgo Cluster [Skillman et al. 1996] which show values of up to 9.4 dex).

Finally there is another important result. As previously said, the fluxes seem to be very odd showing low values of the Balmer decrement. Although the galaxies with these low values do not show any discrepancy in the [OIII]λ5007/[OIII]λ4959 and [NII]λ6583/[NII]λ6548 ratios, there are other galaxies for which these ratios are as large as 5.9 (NGC 3669). In order to check the reliability of the abundance values, a new metallicity was determined where the [OIII]λ5007/[OIII]λ4959 ratio was forced to be 3. The new value of the abundance does not differ by more than the nominal uncertainties from the ones listed in Table 4. Therefore, the oxygen abundances determined in this investigation are very robust.

6. DISCUSSION

As previously said, UGC 7861 shows a very large ([NII])/Hα ratio. In order to check if these values are normal for this sample of galaxies, the diagnostic

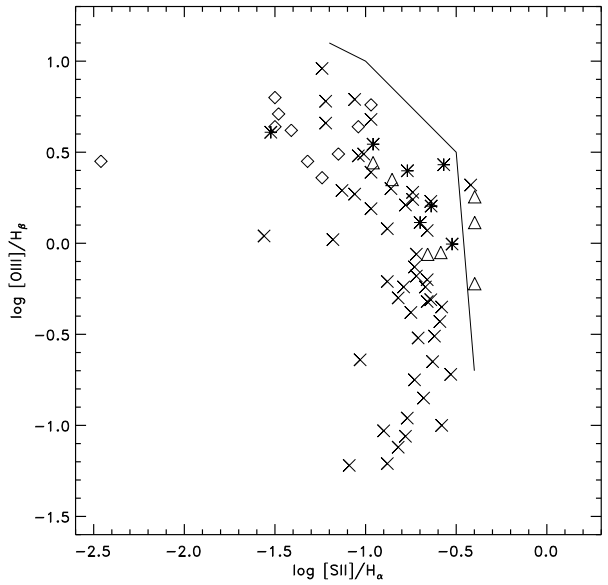

Fig. 5. The [OIII]/Hβ vs. [SII]/Hα diagram for late-type galaxies. Symbols as in Figure 4.

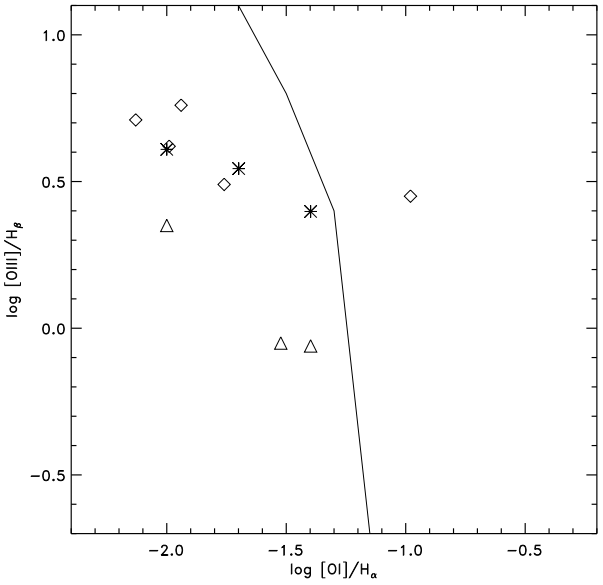

Fig. 6. The [OIII]/Hβ vs. [OI]/Hα diagram for late-type galaxies. Symbols as in Figure 4.

diagrams can be studied. The diagnostic diagrams presented by Baldwin et al. (1981) are based on the [OII]/[OIII] ratio. As we have used the intensity of the [OIII] line to determine the intensity of the [OII] line, we preferred not to use any of these diagrams. Instead, we will consider the diagrams presented by Veilleux & Osterbrock (1987). Figure 4 shows the log([OIII])/Hβ vs. log([NII])/Hα. Along with the data from the galaxies studied in this investigation, we included data from a sample of Im galaxies (Hidalgo-Gámez & Olofsson 2002, and references therein; Hidalgo-Gámez 2006, 2007), from the sample of dS published in HG04, and the Sm galaxies from McCall et al. (1985), named Sp in Hidalgo-Gámez & Olofsson (2002). Although this investigation is about 35 years old, its data still hold. The solid line is the division between the AGN and the normal HII galaxies, according to Veilleux & Osterbrock (1987). Only UGC 7861 among the small galaxies and other three Sp galaxies are inside the AGN locus. The other diagnostic diagrams can be explored in order to see if those galaxies are real AGN, or if there is another explanation for the large [NII]/Hα ratio.

Figure 5 shows the log([OIII])/Hβ vs. log([SII])/Hα diagram. The HII region locus is very well defined by the Sp galaxies from McCall et al. (1985) sample (crosses) and only three Sm and one Sp are located beyond the division line. It is interesting to notice that there is no difference between the Im and the spiral galaxies in this diagram. It is supposed that the spiral arms increase the [SII]/Hα ratio due to the shock waves (see the classical work of Roberts 1969), but such effect is not detected in the dS galaxies. This might be an indication of the absence of shock waves in these galaxies.

Finally, Figure 6 shows the log([OIII])/Hβ vs. log([OI])/Hα diagram. As there is no information on the [OI]λ6300 line intensity for Sp galaxies (see McCall et al. 1985), the HII region locus is not very well defined. Actually, there are only 11 data points in this diagram, five Im and six spirals, which is a very small sample. Anyhow, none of the galaxies but one irregular are inside the AGN locus in this plot.

Then, only UGC 7861 might be an AGN candidate. As said, Moustakas et al. (2010) classified this galaxy as Star Forming on the basis of the log[NII]/Hα ratio alone. Moreover, it is classified as peculiar at NED but its SDSS spectrum does not show any peculiarity in the AGN sense (e.g., broad recombination lines). Also the [OIII])/Hβ ratio is very small, which is another indicator of the absence of an AGN (Osterbrock & Pogge 1985). Finally, in the spectra published by Gil de Paz (2007) there is no indication of an AGN embedded in the galaxy. Most of them show low intensities of the [SII] and [NII] lines but #7. Therefore, it can be concluded that the large [NII])/Hα ratio of this galaxy is not because of its AGN nature but due to shocks or some other phe-

TABLE 5

OXYGEN ABUNDANCES OF dS GALAXIES, REPORTED IN THE LITERATURE ($t > 2004$)

Galaxy	12+log(O/H)	Reference
NGC 625	7.69–8.37	S08
NGC 2552	8.18–8.44	PT07
UGCA 322	8.2	PT07
UGC 5666	7.83–7.99	C09
UGC 5692	7.95	C09
NGC 3510	8.59	KJG05
UGC 7861	7.79–8.53	GP07
UGC 7861	8.43–9.06	M10
UGCA 294	8.21–8.43	SKLC05
UGCA 442	7.72	S08

The name of the galaxy is presented in Column 1, the abundance value in Column 2. References are given in Column 3: S08 stands for Saviane et al. (2008), PT07 for Pilyugin & Thuan (2007), C09 for Crox et al. (2009), KJG05 for Kewley et al. (2005), GP07 for Gil de Paz et al. (2007), M10 for Moustakas et al. (2010), PTh07 for Pilyugin & Thuan (2007), and SKLC05 for Shi et al. (2005).

nomena which increase the nitrogen line intensity. However, its luminosity is higher than expected for its rotational velocity, being located very far outside in the Tully-Fisher relationship (Cárdenas-Martínez 2011).

The log([OIII])/Hβ vs. log([NII])/Hα diagram is quite interesting because it has also been recently used as a metallicity discriminator (Asari et al. 2007), with abundances increasing towards the left-bottom part of the diagram. This is clear in this figure, where the galaxies with the higher abundances are located towards the bottom of the diagram. Also, it can be seen that four of the galaxies studied in this investigation have oxygen abundances quite similar to the Im galaxies, lower than 8.4 dex, while the rest of the galaxies are more metallic, similar to solar. These results are in agreement with those obtained in the previous section.

6.1. *Comparison with other investigations*

As previously noted, three of these galaxies, UGCA 294, UGCA 322, and UGC 7861, have already published information on their abundances. Shi et al. (2005) obtained a value of 12+log(O/H)=8.28 dex with the standard method for UGCA 294. As said in § 4.1, the standard method abundance of UGC 294 obtained here might be too low, but the values determined with the semi-empirical methods are very similar to the abundances reported by Shi et al. (2005). Therefore, it can be concluded that the standard abundance is not real, but due to an overestimation of the [OIII]λ4363 line, and that the oxygen abundance of this galaxy is similar to the SMC.

Concerning UGC 7861, Moustakas et al. (2010) obtained an oxygen abundance between 9.06 dex and 8.43 dex for UGC 7861 and Gil de Paz et al. (2007) determined abundances between 7.79 and 8.53 dex, in both cases with several semi-empirical methods (see Table 3). Gil de Paz et al. (2007) observed HII regions mainly in the XUV disk while the SDSS spectrum stems from the central part of the galaxy, as does the spectrum from Moustakas et al. (2010). Therefore, the higher abundances obtained in these two investigations are expected. Finally, an abundance of 8.2 dex is reported by Pilyugin & Thuan (2007) for UGCA 322, which is very similar to the value obtained in this investigation.

As mentioned in the introduction, there are already 18 dS galaxies with abundance determinations, although most of them were not classified as dS by the authors. In HG04 it is concluded, based on nine dS galaxies (see their Table 4), that their oxygen abundances are closer to the Im galaxies values, with normal spirals having, in general, higher abundances (Dutil 1998). In recent years, the oxygen abundances for another nine galaxies have been determined (Table 5), which confirm the results of HG04, ranging from 8.59 dex in NGC 3510 (Kewley, Jassen, & Geller 2005) to 7.69 dex in NGC 625 (Saviane et al. 2008). For most of them, the abundances were not determined with the standard method, but with any of the semi-empirical methods, as in the present investigation. For two galaxies (NGC 2552 and UGCA 294) more than one of those methods were used in the determination of the oxygen abundances. And another three galaxies (NGC 5666, UGC 7861 and NGC 625) have abundances values determined for several of their HII regions. With the new abundances determined here the conclusion of HG04 still holds completely, because there is only one dS galaxy with oversolar abundance. It is also important to notice that there is no galaxy with an abundance lower than 7.8 dex, but this might be an artifact of the semi-empirical methods (see Hidalgo-Gámez & Ramírez-Fuentes 2009, for details).

6.2. *The role of nitrogen*

As an interesting aside, we will discuss the log(N/O) vs. 12+log(O/H) diagram. This is consid-

TABLE 6

THE log(N/O) RATIO FOR THE GALAXIES OF THE SAMPLE STUDIED HERE

Galaxy	12+log(O/H)	log(N/O)
NGC 3669	8.7±0.09	−0.31±0.03
NGC 5630	8.76±0.10	−0.21±0.02
UGC 7861	8.82±0.07	−0.21±0.03
UGC 8285	8.4±0.01	−1.21±0.1
UGC 9597	8.6±0.03	−0.98±0.1
UGC 1693	8.65±0.02	−0.66±0.07
UGC 6399	8.82±0.05	0.12±0.02
UGC 9381	8.4±0.1	−1.05±0.1
UGC 5242	8.1±0.01	−1.25±0.1
UGCA 322	8.1±0.01	−1.20±0.1
UGC 3947	8.55±0.3	−0.83±0.09
UGC 6205	8.5±0.02	−0.84±0.08
UGC 9542	8.15±0.03	−1.21±0.1
UGC 9018	8.0±0.03	−1.84±0.2
UGC 9018	8.0±0.03	−1.74±0.2
UGCA 294	8.1±0.06	−1.56±0.15
UGCA 294	7.15±0.06	−1.4±0.1

The name of the galaxy is presented in Column 1, the abundance value in Column 2. Columns 3 shows the value of the log(N/O). Two values are presented for UGC 9018 and UGCA 294, the first one determined as described in the text and the second one determined from the electron temperature. The differences for these two galaxies are similar to the estimated errors.

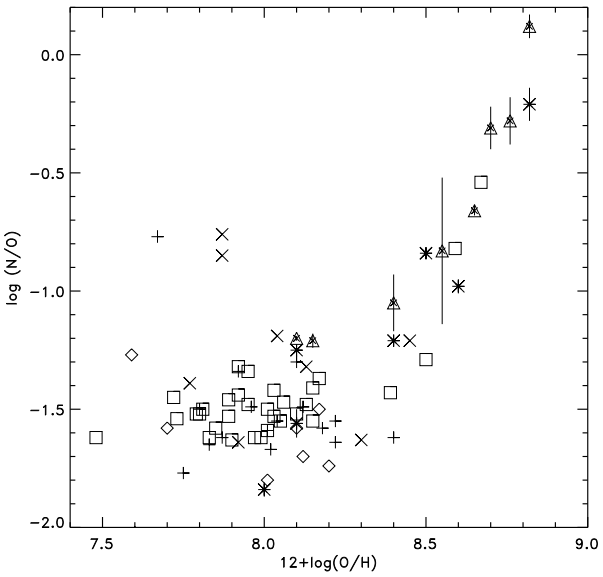

Fig. 7. The log(N/O) vs. 12+log(O/H) diagram for late-type galaxies. Squares are BCG, pluses LSBGs, diamonds dwarf irregulars, crosses are late-type spirals. The galaxies studied in this investigation are represented by stars (dS) and triangles (Sm). The latter ones are plotted along with their uncertainties. The secondary track is clearly defined for high-metallicity galaxies while the low-metallicity galaxies show a scatter diagram with a large dispersion.

ered to be an evolutionary diagram in the sense that oxygen is released into the ISM at an earlier phase than nitrogen, and therefore this ratio is smaller for recent events of star-formation while, as the region ages, the log(N/O) becomes larger (Pilyugin 1992). Even without the [OIII]λ4363 line, the log(N/O) ratio can be obtained (Lee, McCall, & Richer 2003). An electron temperature of the high-ionization zone (T_e^{++}) is determined from the relation between this parameter and the oxygen abundances (e.g., Figure 7 at McGaugh 1991). With this value, equations in Table 1 in Vila-Costas & Edmunds (1993) can be used in order to obtain an electron temperature for the low-ionization zone (T_e^{+}). Finally, the ratio is determined using equation 9 in Pagel et al. (1992). No correction has been applied to the log(N^+/O^+) ratio. These values are tabulated in Table 6, along with their uncertainties.

An important caveat concerns the differences in the log(N^+/O^+) ratio when different values of the abundance are considered, as the abundance is used to determine the T_e^{++} value. Since there are important differences in the abundance determinations, they must affect the log(N^+/O^+) ratio. This point has been checked, and although differences have been found in the ratio, the dispersion among the values is very low, in general. Actually, these have been considered as part of the uncertainties (see Table 6).

The log(N/O) vs. 12+log(O/H) diagram is shown in Figure 7 for all the regions studied here (squares) along with a sample of blue compact galaxies, low-surface brightness, dwarf irregular and Sp from Hidalgo-Gámez & Olofsson (2002, and references therein). It is claimed that nitrogen is a secondary element in spiral galaxies (e.g., Díaz et al. 1991; Pagel 2003; Serrano & Peimbert 1983), being related with the oxygen abundance, while it is primary in irregulars, showing a flat relation with the metallicity (Izotov et al. 2006). This is not at all the situation shown in the diagram (see Figure 7). For metallicities higher than 8.3 dex there is a very clear and steep relation (with a regression coefficient of 0.94), indicating a secondary behavior of nitrogen, irrespective of the morphological type. Actually, in

addition to the Sm and dS, there are three BCG and two Sp in this part of the diagram. For lower values of the abundance, a flat relation can be seen but with a very large dispersion, at least 0.3 dex. This could be seen also as mostly a scatter diagram, with all types of galaxies there, due to the data-points in the low-metallicity and high log(N/O) region (at the top-left of the figure).

Then, it can be concluded that the secondary origin for nitrogen is related to the oxygen abundances only, and not to the morphological type, because there are HII regions in spiral galaxies with log(N/O) lower than −1.5. However, it cannot be said that nitrogen in spiral galaxies is always secondary (Serrano & Peimbert 1983), but only in those HII regions of high abundance. The consideration of nitrogen as a secondary element in spiral galaxies might be only due to the lack of low abundance regions detected up to now in them. Though some authors consider that nitrogen is a primary element in spiral galaxies (Edmunds & Pagel 1984) or a mixture of primary-secondary (Alloin et al. 1979), the data presented in this investigation add evidence of the combined origin of nitrogen (primary/secondary) in spiral galaxies. In any case, the situation of the origin of nitrogen is very complex due to the time delay between the release of nitrogen and oxygen (Pilyugin 1992), the inflow of primordial material that can alter the ratio (Tinsley 1980), or even the existence of a metal-dependent yield which might remove the primary behavior of nitrogen (Vila-Costas & Edmunds 1993).

7. CONCLUSIONS

New oxygen abundances have been determined for seven dS and eight Sm galaxies using spectra from the DR7 of the SDSS data-base. For three galaxies, the standard method can be used because the forbidden oxygen line [OIII] λ4363 was detected. The oxygen abundance determined for two of these galaxies is too low, and not in agreement with the values obtained with other methods. This could be due to a false detection of the forbidden oxygen line at λ4363 Å, which makes the electron temperature higher than the real value. For the third galaxy the metallicity is low, about 8.0 dex, but in the range of the SMC abundances. For all the galaxies four different semi-empirical methods were used. It should be noticed that for 12 galaxies these are the first abundance determinations published.

From these results several conclusions can be obtained:

1. Dwarf spiral galaxies show, in general, solar or undersolar abundances. Only one out of seven dS galaxies has oversolar abundances, less than 15%. On the contrary, normal Sm galaxies usually have solar or oversolar abundances (about 75%), with only two out of eight galaxies having abundances lower than the LMC.

2. The standard metallicities for two (out of three) galaxies were quite unrealistic, with values of about 7.0 dex. This could be due to a overestimation of the [OIII]λ4363 intensity due to noisy spectra.

3. UGC 7861 is quite an intriguing object. Based on the position on the diagnostic diagrams and on the spectral characteristics exhibited, it is concluded that UGC 7861 is not an AGN, as suspected due to its large log([NII]/Hα) ratio. However, this galaxy is much too luminous for its rotation velocity, but of low metallicity for its luminosity.

4. The nitrogen behavior in (spiral) galaxies depends on the metallicity. It is secondary for all the galaxies with abundances higher than 8.3 dex and it is primary for galaxies with lower abundances, whatever the morphological type of the mother galaxy.

5. Despite the odd fluxes found for some galaxies, with an [OIII]λ5007/[OIII]λ4959 ratio different from the canonical value of 2.9, the abundances determined with the semi-empirical methods are quite robust.

Part of the work presented here is based on the Bachelor thesis of A. Moranchel-Basurto and the Servicio Social of A. F. González-Fajardo. The authors thank J. Brenan for English grammar corrections. A. M. H-G. thanks J. R. O'Dell and J. M. Vílchez for interesting discussions on the SDSS data. This investigation is supported by SIP-IPN grant 20121135 and Conacyt-2011-CB165584.

REFERENCES

Aller, L. H. 1984, Physics of Thermal Gaseous Nebulae (Dordrecht: Reidel)
Alloin, D., Collin-Souffrin, S., Joly, M., & Vigroux, L. 1979, A&A, 78, 200
Asari, N. V., et al. 2007, MNRAS, 381, 263
Baldwin, J. A., Phillips, M. M., & Terlevich, R. 1981, PASP, 93, 5
Brocklehurst, M. 1971, MNRAS, 153, 471
Cárdenas-Martínez, N. 2011, BS Thesis, Instituto Politécnico Nacional, Mexico
Carroll, B. W., & Ostlie, D. A. 2007, An Introduction to Modern Astrophysics (2nd ed.; San Francisco: Pearson Education Inc.)
Crox, K. V., et al. 2009, ApJ, 705, 723
de Vaucouleurs, G., de Vaucouleurs, A., Corwin, H. G., Jr., Bura, R. J., Paturel, G., & Fouque, P. 1991, Third Reference Catalogue of Bright Galaxies (New York: Springer-Verlag)

Denicoló, G., Terlevich, E., & Terlevich, R. 2002, MNRAS, 330, 69
Díaz, A. I., Terlevich, E., Vilchez, J. M., Pagel, B. E. J., & Edmunds, M. G. 1991, MNRAS, 253, 245
Dutil, Y. 1998, in ASP Conf. Ser. 147, Abundance Profiles: Diagnostic Tools for Galaxy History, ed. D. Friedli, M. Edmunds, C. Robert, & L. Drissen (San Francisco: ASP), 73
Edmunds, M. G., & Pagel, B. E. J. 1984, MNRAS, 211, 507
Edmunds, M. G., & Roy, J.-R. 1993, MNRAS, 261, L17
Erb, D. K., Shapley, A. E., Pettini, M., Steidel, C., Reddy, N., & Adelberger, K. 2006, ApJ, 644, 813
Fouque, P., Gourgoulhon, E., Chamaraux, P., & Paturel, G. 1992, A&AS, 93, 211
Garcia, A. M. 1993, A&As, 100, 47
Gil de Paz, A., et al. 2005, ApJ, 627, L29
Gil de Paz, A., et al. 2007, ApJ, 661, 115
Hidalgo-Gámez, A. M. 2004, RevMexAA, 40, 37 (HG04)
_____. 2006, AJ, 131, 2078
_____. 2007, AJ, 134, 1447
Hidalgo-Gámez, A. M., & Olofsson, K. 2002, A&A, 389, 836
Hidalgo-Gámez, A. M., & Ramírez-Fuentes, D. 2009, AJ, 134, 169
Izotov, Y. I., Stasińska, G., Meynet, G., Guseva, N. G., & Thuan, T. X. 2006, A&A, 448, 955
Kewley, L. J., Jassen, R. A., & Geller, M. A. 2005, PASP 117, 227
Kniazev, A. Y., Pustilnik, S. A., Grebel, E. K., Lee, H., & Pramskij, A. G. 2004, ApJS, 153, 429
Kobulnicky, H. A., Kennicutt, R. C., Jr., & Pizagno, J. L. 1999, ApJ, 514, 544
Kong, X., & Cheng, F. Z. 2002, A&A, 389, 845
Lee, H., McCall, M. L., & Richer, M. G. 2003, AJ, 125, 2975
Márquez, I., Masegosa, J., Moles, M., Varela, J., Bettoni, D., & Galletta, G. 2002, A&A, 393, 389
Martín-Manjón, M. L., Mollá, M., Díaz, A. I., & Terlevich, R. 2008, MNRAS, 385, 854
McCall, M. L., Rybski, P. M., & Shields, G. A. 1985, ApJS, 57, 1
McGaugh, S. S. 1991, ApJ, 380, 140
Moustakas, J., Kennicutt, R. C., Jr., Tremonti, C. A., Dale, D. A., Smith, J.-D. T., & Calzetti, D. 2010, ApJS, 190, 233
Nilson, P. 1973, Uppsala General Catalogue of Galaxies (Uppsala: Astronomiska Observatorium)
O'Dell, C. R., Ferland, G. J., Porter, R. L., & van Hoof, P. A. M. 2011, ApJ, 733, 9
Olofsson, K. 1997, A&A, 321, 290
Osterbrock, D. E. 1989, Astrophysics of Gaseous Nebulae and Active Galactic Nuclei (Mill Valley, CA: University Science Books)
Osterbrock, D. E., & Pogge, R. W. 1985, ApJ, 297, 166
Pagel, B. E. 2003, Nucleosynthesis and Chemical Evolution of Galaxies (Cambridge: Cambridge Univ. Press)
Pagel, B. E. J.,Edmunds, M. G., Blackwell, D. E., Chun, M. S., & Smith, G. 1979, MNRAS, 189, 95
Pagel, B. E. J., Simonson, E. A., Terlevich, R. J., & Edmunds, M. G. 1992, MNRAS, 255, 325
Pettini, M., & Pagel, B. E. J. 2004, MNRAS, 348, L59
Pilyugin, L. S. 1992, A&A, 260, 58
_____. 2001, A&A, 369, 594
Pilyugin, L. S., & Thuan, T. X. 2005, ApJ, 631, 231
_____. 2007, ApJ, 669, 299
Reaves, G. 1956, AJ, 61, 69
Reyes-Pérez, J. 2009, BS Thesis, Instituto Politécnico Nacional, Mexico
Reyes-Pérez, J., & Hidalgo-Gámez, A. M. 2008, in IAU Symp. 255, Low-Metallicity Star Formation: From First Stars to Dwarf Galaxies, ed. L. K. Hunter, S. C. Manden, & R. Schneider (Cambridge: Cambridge Univ. Press), s/p
Roberts, W. W. 1969, ApJ, 158, 123
Rodriguez, M., & Rubin, R. H. 2003, arXiv:astro-ph/0312246
Sandage, A., Binggeli, B., & Tammann, G. A. 1985, AJ, 90, 1759
Savage, B. D., & Mathis, J. S. 1979, ARA&A, 17, 73
Saviane, I., Ivanov, V. D., Held, E. V., Alloin, D., Rich, R. M., Bresolin, F., & Rizzi, L. 2008, A&A, 487, 901
Schombert, J. M., Pildis, R. A., Eder, J. A., & Oemler, A., Jr. 1995, AJ, 110, 2067
Serrano, A., & Peimbert, M. 1983, RevMexAA, 8, 117
Shi, F., Kong, X., Li, C., & Cheng, F. Z. 2005, A&A, 437, 849
Skillman, E. D., Kennicutt, R. C., Jr., Shields, G. A., & Zaritsky, D. 1996, ApJ, 462, 147
Stasińska, G. 2008, in IAU Symp. 255, Low-Metallicity Star Formation: From First Stars to Dwarf Galaxies, ed. L. K. Hunter, S. C. Manden, & R. Schneider (Cambridge: Cambridge Univ. Press), 375
Tinsley, B. 1980, Fundam. Cosmic Phys., 5, 287
Veilleux, S., & Osterbrock, D. E. 1987, ApJS, 63, 295
Vila-Costas, M. B., & Edmunds, M. G. 1993, MNRAS, 265, 199
Vorontsov-Velyaminov, B. 1974, Observatory, 94, 319
Whiting, A. B., Hau, G. K., Irwing, M., & Verdugo, M. 2007, AJ, 133, 715

A. M. Hidalgo-Gámez, A. Moranchel-Basurto, and A. F. González-Fajardo: Departamento de Física, ESFM-IPN, México, Mexico (ahidalgo, amoranchel@esfm.ipn.mx).